A Finite Volume Scheme with the Discrete Maximum Principle for Diffusion Equations on Polyhedral Meshes

Alexey Chernyshenko and Yuri Vassilevski

Abstract We present a cell-centered finite volume (FV) scheme with the compact stencil formed mostly by the closest neighboring cells. The discrete solution satisfies the discrete maximum principle and approximates the exact solution with second-order accuracy. The coefficients in the FV stencil depend on the solution; therefore, the FV scheme is nonlinear. The scheme is applied to the steady state diffusion equation discretized on a general polyhedral mesh.

1 Introduction

We present a new monotone FV method for the 3D diffusion equation with anisotropic coefficients based on a nonlinear multi-point flux approximation scheme. It satisfies the discrete maximum principle (DMP), works for full anisotropic diffusion tensors and on polyhedral meshes, provides the second order accuracy and has a compact stencil. The basic idea of our approach belongs to LePotier [7] who proposed a monotone FV scheme with a nonlinear two-point flux approximation for the discretization of parabolic equations on triangular meshes. The method was extended to steady-state diffusion problems with full anisotropic tensors on general meshes [4, 8, 11]. For a comprehensive review of nonlinear FV methods we refer to [5]. Recently a new cell-centered minimal stencil FV method with DMP was proposed for full diffusion tensors and unstructured conformal polygonal 2D meshes [9]. The

A. Chernyshenko (✉) · Y. Vassilevski
Institute of Numerical Mathematics, Gubkina 8, Moscow, Russia
e-mail: chernyshenko.a@gmail.com

A. Chernyshenko
Institute of Nuclear Safety, B.Tulskaya 52, Moscow, Russia

Y. Vassilevski
Moscow Institute of Physics and Technology, Institutski 9, Dolgoprudny, M.R., Russia
e-mail: yuri.vassilevski@gmail.com

J. Fuhrmann et al. (eds.), *Finite Volumes for Complex Applications VII - Methods and Theoretical Aspects,* Springer Proceedings in Mathematics & Statistics 77,
DOI: 10.1007/978-3-319-05684-5_18,

3D extension of the method was proposed in [3], the similar algorithm was proposed independently in [6]. In this paper, we demonstrate the properties of the 3D method from [3] on the set of benchmark problems [1]. The FV scheme works on general polyhedral meshes and satisfies DMP in contrast to nonlinear two-point FV scheme from [4], which provides only non-negativity of the discrete solution.

2 Steady State Diffusion Equation

Let Ω be a three-dimensional polyhedral domain with boundary Γ.We consider a model diffusion problem for unknown concentration c:

$$\begin{aligned} -\mathrm{div}(\mathbb{K}\nabla c) &= g \quad \text{in} \quad \Omega \\ c &= g_D \quad \text{on} \quad \Gamma_D \\ -\mathbf{n}\cdot\mathbb{K}\nabla c &= g_N \quad \text{on} \quad \Gamma_N, \end{aligned} \tag{1}$$

where $\Gamma = \Gamma_D \cup \Gamma_N$, $\Gamma_D \neq \emptyset$, $\mathbb{K}(\mathbf{x}) = \mathbb{K}^T(\mathbf{x}) > 0$ is a diffusion tensor, g is a source term and $\mathbf{n}$ is the exterior normal vector.

We consider a conformal polyhedral mesh $\mathscr{T}$ composed of shape-regular cells with planar faces. We assume that each cell is a star-shaped 3D domain with respect to its barycenter. For simplicity, we assume that the diffusion tensor $\mathbb{K}(\mathbf{x})$ is constant inside each cell; however it may jump across mesh faces as well as may change orientation of principal directions.

We denote by $\mathscr{F}_I$, $\mathscr{F}_B$ disjoint sets of interior and boundary faces, respectively. The subset $\mathscr{F}_J \subset \mathscr{F}_I$ collects faces with jumping tensor. Let $\mathscr{F}_T$ denote the sets of faces of polyhedron T. The set $\mathscr{F}_B$ is further split into subsets $\mathscr{F}_B^D$ and $\mathscr{F}_B^N$ where the Dirichlet and Neumann boundary conditions, respectively, are imposed.

3 Nonlinear FV Scheme

The FV scheme uses one degree of freedom, C_T, per cell T collocated at $\mathbf{x}_T$, the barycenter of the cell. For every face $f \in \mathscr{F}_I \cup \mathscr{F}_B$, we denote the face barycenter by $\mathbf{x}_f$ and associate a collocation point with $\mathbf{x}_f$ for $f \in \mathscr{F}_B$.

We shall refer to collocation points on faces as the auxiliary collocation points. They are introduced for mathematical convenience and will not enter the final algebraic system although will affect system coefficients. In contrast, we shall refer to the other collocation points as the primary collocation points whose discrete concentrations form the unknown vector in the algebraic system.

For every cell T we define a set Σ_T of nearby collocation points. First, we add to Σ_T the collocation point $\mathbf{x}_T$. Then, for every face $f \in \mathscr{F}_T \setminus (\mathscr{F}_J \cup \mathscr{F}_B)$, we add the

collocation point $\mathbf{x}_{T'_f}$, where T'_f is the cell sharing f with T. Finally, for boundary faces $f \in \mathscr{F}_T \cap \mathscr{F}_B$, we add the collocation point $\mathbf{x}_f$.

Let $\mathbf{q} = -\mathbb{K}\nabla c$ denote the flux which satisfies the mass balance equation:

$$\operatorname{div} \mathbf{q} = g \quad \text{in} \quad \Omega. \tag{2}$$

A cell-centered FV scheme is derived by integrating Eq. (2) over a polyhedral cell T and using the Green's formula:

$$\int_{\partial T} \mathbf{q} \cdot \mathbf{n}_T \, \mathrm{d}s = \int_T g \, \mathrm{d}x, \tag{3}$$

where $\mathbf{n}_T$ denotes the external unit normal to ∂T. Let f denote a face of cell T and $\mathbf{n}_f$ be the corresponding normal vector. It will be convenient to assume that $|\mathbf{n}_f| = |f|$, where $|f|$ denotes the area of face f. The Eq. (3) becomes

$$\sum_{f \in \partial T} \mathbf{q}_f \cdot \mathbf{n}_f = \int_T g \, \mathrm{d}x, \tag{4}$$

where $\mathbf{q}_f$ is the average flux density for face f.

3.1 Diffusive Flux in Homogeneous Anisotropic Medium

Let us first consider a homogeneous medium. We assume that for every cell-face pair $T_i \in \mathscr{T}$, $f \in \mathscr{F}_{T_i}$, there exist three points $\mathbf{x}_{f,j}$, $\mathbf{x}_{f,k}$, and $\mathbf{x}_{f,l}$ in set Σ_{T_i} such that the following condition holds: the co-normal vector $\boldsymbol{\ell}_f = \mathbb{K}(\mathbf{x}_f)\mathbf{n}_f$ started from $\mathbf{x}_{T_i}$ belongs to the trihedral corner formed by vectors

$$\mathbf{t}_{ij} = \mathbf{x}_{f,j} - \mathbf{x}_{T_i}, \quad \mathbf{t}_{ik} = \mathbf{x}_{f,k} - \mathbf{x}_{T_i}, \quad \mathbf{t}_{il} = \mathbf{x}_{f,l} - \mathbf{x}_{T_i}, \tag{5}$$

and

$$\ell_f = \alpha_{ij}\mathbf{t}_{ij} + \alpha_{ik}\mathbf{t}_{ik} + \alpha_{il}\mathbf{t}_{il}, \tag{6}$$

where $\alpha_{ij} > 0$, $\alpha_{ik} \geq 0$, $\alpha_{il} \geq 0$. We assume that the first point, $\mathbf{x}_{f,j}$, belongs to the cell T_j which shares f with T_i. If Σ_{T_i} does not contain the desired points, one can extend Σ_{T_i} with other neighbors of T_i. This extension leads to increasing the minimal stencil. The algorithm of a search of such points is described in [4].

Recalling the definition of the diffusive flux and using finite differences to approximate directional derivatives, we obtain:

$$\begin{aligned} \mathbf{q} \cdot \mathbf{n}_f &= -\nabla c \cdot (\mathbb{K}_{T_i} \mathbf{n}_f) = -\alpha_{ij}\nabla c \cdot \mathbf{t}_{ij} - \alpha_{ik}\nabla c \cdot \mathbf{t}_{ik} - \alpha_{il}\nabla c \cdot \mathbf{t}_{il} \\ &= -\alpha_{ij}(C_{T_j} - C_{T_i}) - \alpha_{ik}(C_{T_k} - C_{T_i}) - \alpha_{il}(C_{T_l} - C_{T_i}) + O(|f|). \end{aligned} \tag{7}$$

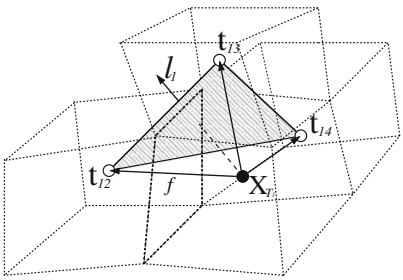

Fig. 1 Co-normal vector ℓ_f belongs to the trihedral corner formed by $\mathbf{t}_{12}, \mathbf{t}_{13}, \mathbf{t}_{14}$

The numerical diffusive flux is obtained by dropping out the term $O(|f|)$.

Setting $i = 1$, $j = 2$, $k = 3$, $l = 4$ in (7) (see Fig. 1) we obtain a numerical diffusive flux $q_f^{(1)}$ from cell T_1 to cell T_2 through their common face f. Similarly, setting $i = 2$, $j = 1$, $k = 5$, $l = 6$ in (7) and assuming that $-\ell_f$ started from $\mathbf{x}_{T_2}$ belongs to the trihedral corner formed by vectors $\mathbf{t}_{21}, \mathbf{t}_{25}, \mathbf{t}_{26}$, we obtain a different numerical flux, $q_f^{(2)}$, in the opposite direction. The final numerical flux is a linear combination of these two fluxes:

$$\begin{aligned} q_f &= \mu_1 q_f^{(1)} + \mu_2(-q_f^{(2)}) \\ &= \mu_1(\alpha_{12}(C_{T_1} - C_{T_2}) + \alpha_{13}(C_{T_1} - C_{T_3}) + \alpha_{14}(C_{T_1} - C_{T_4})) \\ &\quad - \mu_2(\alpha_{21}(C_{T_2} - C_{T_1}) + \alpha_{25}(C_{T_2} - C_{T_5}) + \alpha_{26}(C_{T_2} - C_{T_6})). \end{aligned} \tag{8}$$

In [4] the weights μ_1 and μ_2 are selected to obtain the two-point discretization. In this work they are selected to balance the relative contribution of the left and the right fluxes to the final flux. The second requirement is to approximate the true flux. These requirements lead us to the following system

$$\begin{aligned} q_f^{(1)}\mu_1 + q_f^{(2)}\mu_2 &= 0, \\ \mu_1 + \mu_2 &= 1. \end{aligned} \tag{9}$$

If $|q_f^{(1)}| + |q_f^{(2)}| = 0$, the solution of these two equations is not unique and we set $\mu_1 = \mu_2 = 1/2$. Otherwise, we have $|q_f^{(1)}| + |q_f^{(2)}| \neq 0$ and must consider two cases. In the first case $q_f^{(1)} q_f^{(2)} \leq 0$ and the solution is

$$\mu_1 = \frac{|q_f^{(2)}|}{|q_f^{(1)}| + |q_f^{(2)}|}, \quad \mu_2 = \frac{|q_f^{(1)}|}{|q_f^{(1)}| + |q_f^{(2)}|}. \tag{10}$$

Thus,

$$q_f = \frac{2q_f^{(1)}|q_f^{(2)}|}{|q_f^{(1)}| + |q_f^{(2)}|} = -\frac{2q_f^{(2)}|q_f^{(1)}|}{|q_f^{(1)}| + |q_f^{(2)}|} \tag{11}$$

and the diffusive flux has two equivalent algebraic representations:

$$\begin{aligned} q_f &= 2\mu_1(\alpha_{12}(C_{T_1} - C_{T_2}) - \alpha_{13}(C_{T_1} - C_{T_3}) - \alpha_{14}(C_{T_1} - C_{T_4})) \\ &= A_{12}(C_{T_1} - C_{T_2}) + A_{13}(C_{T_1} - C_{T_3}) + A_{14}(C_{T_1} - C_{T_4}) \end{aligned} \tag{12}$$

and

$$\begin{aligned} -q_f &= 2\mu_2(\alpha_{21}(C_{T_2} - C_{T_1}) - \alpha_{25}(C_{T_2} - C_{T_5}) - \alpha_{26}(C_{T_2} - C_{T_6})) \\ &= A_{21}(C_{T_2} - C_{T_1}) + A_{25}(C_{T_2} - C_{T_5}) + A_{26}(C_{T_2} - C_{T_6}) \end{aligned} \tag{13}$$

with non-negative coefficients A_{12}, A_{13}, A_{14}, A_{21}, A_{25} and A_{26}. Note that these coefficients depend on the fluxes and hence on the concentrations at neighboring cells. The second case $q_f^{(1)} q_f^{(2)} > 0$ leads to a potentially degenerate diffusive flux. In order to avoid this degeneracy, we re-group the terms in (8) following [11]

$$q_f = \mu_1 \tilde{q}_f^{(1)} + \mu_2(-\tilde{q}_f^{(2)}) + (\mu_1\alpha_{12} + \mu_2\alpha_{21})(C_{T_1} - C_{T_2}), \tag{14}$$

where $\tilde{q}_f^{(1)} = \alpha_{13}(C_{T_1} - C_{T_3}) + \alpha_{14}(C_{T_1} - C_{T_4})$, $\tilde{q}_f^{(2)} = \alpha_{25}(C_{T_2} - C_{T_5}) + \alpha_{26}(C_{T_2} - C_{T_6})$. The coefficients μ_1 and μ_2 are computed by balancing the modified numerical fluxes

$$\tilde{q}_f^{(1)}\mu_1 + \tilde{q}_f^{(2)}\mu_2 = 0$$

and using the convexity condition. Again, if the solution is not unique, we set $\mu_1 = \mu_2 = 1/2$. For the case $\tilde{q}_f^{(1)}\tilde{q}_f^{(2)} \leq 0$ we obtain

$$\begin{aligned} q_f &= 2\mu_1 \tilde{q}_f^{(1)} + (\mu_1\alpha_{12} + \mu_2\alpha_{21})(C_{T_1} - C_{T_2}) \\ &= A_{13}(C_{T_1} - C_{T_3}) + A_{14}(C_{T_1} - C_{T_4}) + A_{12}(C_{T_1} - C_{T_2}) \\ &= -2\mu_2 \tilde{q}_f^{(2)} - (\mu_1\alpha_{12} + \mu_2\alpha_{21})(C_{T_2} - C_{T_1}) \\ &= -A_{25}(C_{T_2} - C_{T_5}) - A_{26}(C_{T_2} - C_{T_6}) - A_{21}(C_{T_2} - C_{T_1}), \end{aligned} \tag{15}$$

where $A_{12} = A_{21} = \mu_1\alpha_{12} + \mu_2\alpha_{21}$. For the case $\tilde{q}_f^{(1)}\tilde{q}_f^{(2)} > 0$, we obtain

$$q_f = (\mu_1\alpha_{12} + \mu_2\alpha_{21})(C_{T_1} - C_{T_2}) = A_{12}(C_{T_1} - C_{T_2}). \tag{16}$$

The coefficients A_{12}, A_{13}, A_{14}, A_{21}, A_{25} and A_{26} in (15), (16) are non-negative by construction and depend on the concentrations.

We use the Dirichlet boundary data on faces $f \in \mathscr{F}_B^D$, $C_f = \int_f g_D ds/|f|$ as the known values of the concentration at points $\mathbf{x}_f$. For the Neumann boundary data on faces $f \in \mathscr{F}_B^N$ we calculate the diffusive flux as $q_f = \overline{g}_{N,f}$, where $\overline{g}_{N,f}$ is the average value of g_N on f.

3.2 Diffusive Flux in Heterogeneous Anisotropic Medium

Let us consider a heterogeneous medium. Let a face $f \in \mathscr{F}_J$ be shared by cells T_1 and T_2. We denote the plane containing f by p_f and consider a continuous piecewise linear function $\mathscr{R}(\mathbf{x})$ such that

$$\mathscr{R}(\mathbf{x}_{T_1}) = C_{T_1}, \quad \mathscr{R}(\mathbf{x}_{T_2}) = C_{T_2}, \tag{17}$$

and the diffusive flux of $\mathscr{R}(\mathbf{x})$ is continuous:

$$\mathbb{K}_{T_1} \nabla \mathscr{R}(\mathbf{x})|_{T_1} \cdot \mathbf{n}_f = \mathbb{K}_{T_2} \nabla \mathscr{R}(\mathbf{x})|_{T_2} \cdot \mathbf{n}_f. \tag{18}$$

Then, there exists a harmonic averaging point $\mathbf{y}_f \in p_f$ and a coefficient $0 \le \alpha_f \le 1$ independent of $\mathscr{R}$ such that [2]:

$$C_f \equiv \mathscr{R}(\mathbf{y}_f) = \alpha_f C_{T_1} + (1 - \alpha_f) C_{T_2}, \tag{19}$$

where

$$\alpha_f = \frac{d_{2,f} \mathbf{n}_f \cdot (\mathbb{K}_{T_1} \mathbf{n}_f)}{d_{2,f} \mathbf{n}_f \cdot (\mathbb{K}_{T_1} \mathbf{n}_f) + d_{1,f} \mathbf{n}_f \cdot (\mathbb{K}_{T_2} \mathbf{n}_f)}, \tag{20}$$

and $d_{i,f}$ is the distance from point $\mathbf{x}_{T_i}$ to plane p_f.

The scheme can be adjusted to discontinuous tensors by using harmonic averaging points. The approximation of the directional derivative $\nabla c \cdot \mathbf{t}_{ij}$ is accurate only inside each material. This limits significantly the number of admissible directions $\mathbf{t}_{ij}$ to the point that expansion (6) does not exist. The additional vectors from collocation points $\mathbf{x}_{T_i}$ and $\mathbf{x}_{T_j}$ to the harmonic point $\mathbf{y}_f$ can be used to find the expansion.

The formula for the final diffusive flux q_f involves both C_{T_i} and C_f, but the latter can be eliminated using the convex combination (19) without increasing the stencil size and preserving the DMP. For example, formula (12) is modified as follows:

$$\begin{aligned} q_f &= A_{12}(C_{T_1} - C_f) + A_{13}(C_{T_1} - C_{T_3}) + A_{14}(C_{T_1} - C_{T_4}) \\ &= A_{12}(1 - \alpha_f)(C_{T_1} - C_{T_2}) + A_{13}(C_{T_1} - C_{T_3}) + A_{14}(C_{T_1} - C_{T_4}). \end{aligned} \tag{21}$$

The other formulas are modified similarly.

3.3 Solution of the System

Let $\mathbf{C}$ be the vector of all cell-centered unknowns. Replacing the fluxes in Eq. (4) by their numerical approximations, we obtain a system of nonlinear equations

$$\mathbf{M}(\mathbf{C})\mathbf{C} = \mathbf{F}(\mathbf{C}). \tag{22}$$

with a square M-matrix **M** and a right hand side vector **F**. The entries of **M** are defined by formulas (12), (13), (15), (16) and (21) and depend on **C**. We note that coefficients from (12) and (13) are landed into the rows of **M** corresponding the cells T_1 and T_2, respectively. The matrix **M** has diagonal dominance in rows, which leads to the DMP. The system is solved by the Picard method or Anderson method [10]. The DMP holds for both the converged solution and each Picard iterate.

4 Numerical Experiments

We verify the convergence and monotonicity properties of the proposed nonlinear FV scheme with a few numerical experiments. We consider 3D benchmark problems from FVCA-6 [1] with corresponding notations.

- **Test 1: Mild anisotropy,** $c(x, y, z) = 1+\sin(\pi x)\sin\left(\pi\left(y+\frac{1}{2}\right)\right)\sin\left(\pi\left(z+\frac{1}{3}\right)\right)$, $\min = 0$, $\max = 2$, **Tetrahedral meshes (B),Voronoi meshes (C), Kershaw meshes(D), Checkerboard meshes (I)**

Mesh	i	nu	nmat	umin	umax	normg	erl2	ratiol2	ergrad	ratiograd
	2	3898	23300	0.003	1.986	1.764	6.23e−03	1.399	2.06e−01	0.872
	3	7711	44504	0.004	1.997	1.771	3.69e−03	2.303	1.67e−01	0.923
B	4	15266	86993	0.002	1.997	1.780	2.81e−03	1.197	1.31e−01	1.066
	5	30480	169809	1e−04	1.998	1.785	1.67e−03	2.258	1.06e−01	0.919
	6	61052	334864	3e−05	1.998	1.789	1.15e−03	1.611	8.66e−02	0.873
	2	66	1159	0.045	1.925	1.627	7.50e−02	−0.054	5.70e−01	1.695
	3	130	2241	0.020	1.967	1.608	3.92e−02	2.871	4.23e−01	1.320
C	4	228	3875	0.020	1.965	1.689	2.56e−02	2.275	3.13e−01	1.608
	5	356	6100	−0.002	1.991	1.689	2.05e−02	1.496	2.50e−01	1.513
	2	4096	33832	0.002	2.000	1.693	6.73e−02	0.398	5.55e−01	0.115
D	3	32768	250058	−0.002	1.996	1.723	4.95e−02	0.443	4.00e−01	0.472
	4	262144	1810432	0.003	1.997	1.761	3.02−03	0.713	2.31e−01	0.792
	2	288	3240	0.050	1.960	1.761	3.32e−02	1.060	3.16e−01	0.989
I	3	2304	23376	0.001	1.995	1.770	9.35e−03	1.828	1.37e−01	1.206
	4	18432	176544	0.002	1.998	1.789	2.79e−03	1.745	5.90e−02	1.215
	5	147456	1369920	1e−04	2.000	1.796	9.23e−04	1.596	2.72e−02	1.117

- **Test 2: Heterogeneous anisotropy,** $c(x, y, z) = x^3y^2z + x\sin(2\pi xz)\sin(2\pi xy)\sin(2\pi z)$, $\min = -0.862$, $\max = 1.0487$, **Prism meshes**

i	nu	nmat	umin	umax	normg	erl2	ratiol2	ergrad	ratiograd
1	1210	14275	−1.006	1.006	3.035	3.36e−02		3.14e−01	
2	8820	92696	−0.971	0.971	3.388	8.29e−03	2.114	1.17e−01	1.491
3	28830	289232	−1.000	1.000	3.492	3.68e−03	2.057	6.07e−02	1.662
4	67240	658039	−0.998	0.998	3.534	2.07e−03	2.038	3.67e−02	1.782

The differential problems of Test 1 and Test 2 do not satisfy the maximum principle since the exact solution has local extrema. Therefore, no numerical scheme can guarantee DMP.

- **Test 4: Flow around a well**, $\min = 0,\ \max = 5.415$, **Well meshes**

i	nu	nmat	umin	umax	normg	erl2	ratiol2	ergrad	ratiograd
3	5016	40585	0.172	5.329	1581.870	1.92e−03	2.765	7.22e−02	2.207
4	11220	87248	0.128	5.330	1603.979	1.18e−03	1.814	4.79e−02	1.529
5	23210	175975	0.097	5.339	1612.048	6.86e−04	2.239	3.20e−02	1.665
6	42633	318146	0.075	5.345	1615.236	4.78e−04	1.782	2.21e−02	1.826
7	74679	551433	0.058	5.361	1617.424	3.39e−04	1.839	1.69e−02	1.436

- **Test 5: Discontinuous permeability,** $c(x, y, z) = a_i \sin(2\pi x) \sin(2\pi y) \sin(2\pi z)$, $\min = -100,\ \max = 100$, **Locally refined meshes**

i	nu	nmat	umin	umax	normg	erl2	ratiol2	ergrad	ratiograd
1	22	124	−209.045	209.045	442.542	1.09e+00		1.00e+00	
2	176	1112	−43.618	43.618	58.442	2.23e−01	2.289	1.80e+00	−0.848
3	1408	9376	−83.042	83.042	89.814	5.76e−02	1.953	3.16e−01	2.510
4	11264	76928	−95.567	95.567	97.224	1.36e−02	2.082	1.53e−01	1.046

The proposed 3D nonlinear FV scheme for the diffusion equation satisfies the discrete maximum principle and has a compact stencil. The scheme provides asymptotic second order accuracy for concentrations except for extremely irregular Kershaw meshes.

Acknowledgments This work has been supported in part by RFBR grants 12-01-33084, 14-01-00830, Russian Presidential grant MK-7159.2013.1, Federal target programs of Russian Ministry of Education and Science, ExxonMobil Upstream Research Company, and project "Breakthrough" of Rosatom.

References

1. FVCA6 3D Benchmark. http://www.latp.univ-mrs.fr/latp_numerique/?q=node/4
2. Agelas, L., Eymard, R., Herbin, R.: A nine-point finite volume scheme for the simulation of diffusion in heterogeneous media. C. R. Acad. Sci. Paris Ser. I. **347**, 673–676 (2009)
3. Chernyshenko, A.: Generation of adaptive polyhedral meshes and numerical solution of 2nd order elliptic equations in 3D domains and on surfaces. Ph.D. thesis, INM RAS, Moscow (2013).
4. Danilov, A., Vassilevski, Y.: A monotone nonlinear finite volume method for diffusion equations on conformal polyhedral meshes. Russ. J. Numer. Anal. Math. Model. **24**(3), 207–227 (2009)
5. Droniou, J.: Finite volume schemes for diffusion equations: introduction to and review of modern methods. Math. Models Methods Appl. Sci. (2014). To appear
6. Gao, Z.M., Wu, J.M.: A small stencil and extremum-preserving scheme for anisotropic diffusion problems on arbitrary 2d and 3d meshes. J. Comp. Phys. **250**, 308–331 (2013)

7. LePotier, C.: Schema volumes finis monotone pour des operateurs de diffusion fortement anisotropes sur des maillages de triangle non structures. C. R. Acad. Sci. Paris Ser. I. **341**, 787–792 (2005)
8. Lipnikov, K., Svyatskiy, D., Shashkov, M., Vassilevski, Y.: Monotone finite volume schemes for diffusion equations on unstructured triangular and shape-regular polygonal meshes. J. Comp. Phys. **227**, 492–512 (2007)
9. Lipnikov, K., Svyatskiy, D., Vassilevski, Y.: Minimal stencil finite volume scheme with the discrete maximum principle. Russ. J. Numer. Anal. Math. Model. **27**(4), 369–385 (2012)
10. Lipnikov, K., Svyatskiy, D., Vassilevski, Y.: Anderson acceleration for nonlinear finite volume scheme for advection-diffusion problems. SIAM J. Sci. Comput. **35**(2), 1120–1136 (2013)
11. Yuan, G., Sheng, Z.: The finite volume scheme preserving extremum principle for diffusion equations on polygonal meshes. J. Comp. Phys. **230**(7), 2588–2604 (2011)